

Least Squares Migration of Synthetic Aperture Data for Towed Streamer Electromagnetic Survey

Xiaolei Tu¹ and Michael S. Zhdanov²

Abstract—Towed streamer electromagnetic (TSEM) survey is an efficient data acquisition technique capable of collecting a large volume of electromagnetic (EM) data over extensive areas rapidly and economically. The TSEM survey is capable of detecting and characterizing marine hydrocarbon (HC) reservoirs. However, interpretation of the TSEM data is still a very challenging problem. We propose solving this problem by migrating the optimal synthetic aperture (OSA) data for the TSEM survey. We first represent the OSA data as a solution of Lippmann–Schwinger equation and then demonstrate that the migration of OSA data is just the inner product of the backward-propagated and forward-propagated EM fields. The migration problem is solved iteratively within the general framework of the reweighted, regularized, conjugate gradient (RRCG) method. The proposed method was tested with two synthetic models. We also applied this method to the TSEM data set collected in the Barents Sea and revealed a resistive layer at a depth of about 500 m.

Index Terms—Electromagnetic (EM), migration, synthetic aperture (SA).

I. INTRODUCTION

THE concept of synthetic aperture (SA) method is based on an idea that a virtual source constructed from different actual sources with specific radiation patterns can steer the combined fields in the direction of the area of interest [1]–[3]. In the letters of Yoon and Zhdanov [4] and Zhdanov *et al.* [5], the authors introduced a concept of optimal synthetic aperture (OSA) by determining the optimal parameters of the SA data, which enhanced the electromagnetic (EM) anomaly from a resistive region located in either deep or shallow marine environments. This method was also extended for rapid imaging of the towed streamer electromagnetic (TSEM) survey data based on the concept of OSA. The OSA method could image the horizontal location of subsurface anomalies in a very rapid way without solving Maxwell’s equations. However, the OSA images do not provide the physical properties (i.e., conductivity or resistivity) of the anomaly. Furthermore, the SA or OSA images do not contain in-depth information on the target since

Manuscript received May 23, 2019; revised January 3, 2020; accepted January 19, 2020. This work was supported in part by the University of Utah Consortium for Electromagnetic Modeling and Inversion, in part by TechnoImaging, LLC, and in part by the Russian Science Foundation (RSF) under Project 16-11-10188. (Corresponding author: Xiaolei Tu.)

Xiaolei Tu is with the Department of Geology and Geophysics, University of Utah, Salt Lake City, UT 84112 USA (e-mail: tuxl2009@hotmail.com).

Michael S. Zhdanov is with the University of Utah, Salt Lake City, UT 84112 USA, also with TechnoImaging, LLC, Salt Lake City, UT 84107 USA, and also with the Moscow Institute of Physics and Technology (MIPT), 141701 Moscow, Russia (e-mail: michael.s.zhdanov@gmail.com).

Color versions of one or more of the figures in this letter are available online at <http://ieeexplore.ieee.org>.

Digital Object Identifier 10.1109/LGRS.2020.2968862

they do not take the survey geometry and frequency range into consideration.

In this letter, we have developed a new approach to imaging the TSEM data by performing migration directly on the OSA data. The developed novel method differs from the previous EM migration algorithms in three aspects. First, we apply the migration to the OSA data rather than to the observed EM data. Second, calculations of the migrated field (or the downward propagation of the time-reversed backscattered fields) in the previous methods required a solution to Maxwell’s equations, which is a nonlinear problem and needs considerable computational efforts. In our approach, the Lippmann–Schwinger equation corresponding to Maxwell’s system is linearized by introducing a new model parameter, which reduces the forward modeling computations significantly. Last but not least, the recovery of the subsurface image of the new model parameter is obtained by a linear iterative solver, which we refer to as the least squares migration after its seismic counterpart.

II. INTEGRAL REPRESENTATIONS OF THE OSA DATA

We consider a typical TSEM survey consisting of a towed bipole transmitter and a set of towed receivers. The transmitter generates a low-frequency EM field from positions with coordinates $\tilde{\mathbf{r}}_j, j = 1, 2, \dots, J$. According to Yoon and Zhdanov [4], the OSA data $d_R^{(l)}$ at the virtual receiver position \mathbf{r}_l are computed as

$$d_R^{(l)} = \frac{d_A^{(l)}}{d_B^{(l)}} = \frac{\sum_{j=1}^J E_j^{(l)} w_j}{\sum_{j=1}^J E_j^{\text{ref}(l)} w_j} \quad (1)$$

where $E_j^{(l)}$ denotes the interpolated field at the virtual receiver position \mathbf{r}_l corresponding to the transmitter located at position $\tilde{\mathbf{r}}_j$. $E_j^{\text{ref}(l)}$ represents the corresponding reference field for $E_j^{(l)}$, which generally depends on the offset $|\mathbf{r}_l - \tilde{\mathbf{r}}_j|$. w_j represents the OSA weight.

Consider a 3-D geoelectrical model with background conductivity σ_b and local inhomogeneity with varying conductivity, $\sigma = \sigma_b + \sigma_a$. The EM field generated by the OSA source in this model can be presented as the sum of the background and anomalous fields

$$\tilde{\mathbf{E}} = \tilde{\mathbf{E}}^b + \tilde{\mathbf{E}}^a. \quad (2)$$

The integral equation for 3-D EM-forward modeling problem is written as

$$\tilde{\mathbf{E}}^a(\mathbf{r}_l) = \iiint_V \mathbf{G}(\mathbf{r}_l | \mathbf{r}) \cdot \{\sigma_a(\mathbf{r})[\tilde{\mathbf{E}}^b(\mathbf{r}) + \tilde{\mathbf{E}}^a(\mathbf{r})]\} dv. \quad (3)$$

According to Zhdanov [6], the anomalous field, $\tilde{\mathbf{E}}^a$, inside the inhomogeneous domain can be projected onto the background field by a scattering tensor, $\hat{\lambda}$

$$\tilde{\mathbf{E}}^a(\mathbf{r}_l) = \iiint_V \mathbf{G}(\mathbf{r}_l | \mathbf{r}) \cdot \{\sigma_a(\mathbf{r})[\hat{\mathbf{I}} + \hat{\lambda}(\mathbf{r})] \cdot \tilde{\mathbf{E}}^b(\mathbf{r})\} dv \quad (4)$$

where $\hat{\mathbf{I}}$ is the identity tensor.

The scattering tensor, $\hat{\lambda}$, is called the electrical reflectivity tensor. In general, it is a second-order tensor with components represented by smoothly varying functions of the coordinates. We should note that the scalar components of $\hat{\lambda}(\mathbf{r})$ are complex functions depending nonlinearly on the anomalous conductivity, the background conductivity, and the excitation source. However, in the case of weak-contrast media, $\hat{\lambda}(\mathbf{r})$ is less dependent on the source and can be assumed to be a function of $\sigma_a(\mathbf{r})$ only. We assume, for simplicity, that $\hat{\lambda}$ is a scalar tensor, $\hat{\lambda} = \lambda \hat{\mathbf{I}}$. Under this assumption, a new model parameter, $m(\mathbf{r})$, which we call modified conductivity, is introduced

$$m(\mathbf{r}) = \sigma_a(\mathbf{r})[1 + \lambda(\mathbf{r})]. \quad (5)$$

By introducing the modified conductivity, $m(\mathbf{r})$, the Lippmann–Schwinger equation can be linearized as follows:

$$\tilde{\mathbf{E}}^a(\mathbf{r}_l) = \iiint_V \mathbf{G}(\mathbf{r}_l | \mathbf{r}) \cdot m(\mathbf{r}) \tilde{\mathbf{E}}^b(\mathbf{r}) dv \quad (6)$$

which can also be written in a compact form

$$\mathbf{d} = \mathbf{Lm} \quad (7)$$

with the linear modeling operator, \mathbf{L} , and the data, \mathbf{d} , defined as the following:

$$\mathbf{L} = \iiint_V \mathbf{G}(\mathbf{r}_l | \mathbf{r}) \cdot \tilde{\mathbf{E}}^b(\mathbf{r}) dv \quad (8)$$

$$\mathbf{d} = [\tilde{\mathbf{E}}^a(\mathbf{r}_1) \quad \tilde{\mathbf{E}}^a(\mathbf{r}_2) \quad \cdots \quad \tilde{\mathbf{E}}^a(\mathbf{r}_L)]^T. \quad (9)$$

We should note that one can treat the OSA data introduced above in (1) are the data considered in (7) and (9): $\mathbf{d} = \mathbf{d}_R$. In other words, we can use the developed integral representation for the OSA data as well.

III. LEAST SQUARES ITERATIVE MIGRATION OF OSA DATA

As demonstrated in Zhdanov [6], migration is the action of the adjoint operator on the observed data. It follows that the migration image of modified conductivity, \mathbf{m}^{mig} , can be introduced as an action of the adjoint operator, \mathbf{L}^* , on the anomalous field data, \mathbf{d} :

$$\mathbf{m}^{\text{mig}} = \mathbf{L}^* \mathbf{d}. \quad (10)$$

It can be proved that the migration operator can be written as follows:

$$\mathbf{L}^* \mathbf{d} = \tilde{\mathbf{E}}^{b*}(\mathbf{r}) \cdot \left[\iiint_S \mathbf{G}^*(\mathbf{r} | \mathbf{r}') d(\mathbf{r}') ds' \right] \quad (11)$$

where $\mathbf{G}^*(\mathbf{r} | \mathbf{r}')$ is the complex conjugate Green's tensor. Considering that the complex conjugate is equivalent to time reverse in the time domain, the complex conjugate Green's

tensor will result in the backward propagation of EM fields in time domain. The term in square brackets in (11) has a physical meaning of the backward propagation of the observed data back toward the subsurface media simultaneously from all the receivers. That is, all the receivers are considered as virtual sources and the observed data are taken as the source function. If we denote this backward-propagated field as

$$\mathbf{E}^{\text{BP}}(\mathbf{r}) = \iiint_S \mathbf{G}^*(\mathbf{r} | \mathbf{r}') d(\mathbf{r}') ds' \quad (12)$$

then, the migration of the EM anomalous field is then the inner product of the backward-propagated and forward-propagated fields

$$\mathbf{m}^{\text{mig}} = \langle \mathbf{E}^{\text{BP}}(\mathbf{r}), \tilde{\mathbf{E}}^b(\mathbf{r}) \rangle. \quad (13)$$

The migrated modified conductivity \mathbf{m}^{mig} never exactly predicts the observed data in the equation $\mathbf{d} = \mathbf{Lm}$. We can find the solution as that minimizing the following regularized sum of the squared residuals:

$$p(\alpha) = \|\mathbf{Lm} - \mathbf{d}\|^2 + \alpha s(\mathbf{m}) \rightarrow \min. \quad (14)$$

The solution of the above minimization problem is called least squares migration after its seismic counterpart. We should also note that the gradient of the least squares migration parametric functional without regularization is exactly the one-step migration image \mathbf{m}^{mig} . The least squares migration is thus an analog (for the case of modified conductivity, \mathbf{m}) of the generalized iterative migration method with regularization. The regularization term incorporates *a priori* information about the model, turning the ill-posed unconstrained inverse problem into a conditionally well-posed inverse problem [6].

Due to the diffusive nature of the low-frequency EM fields, the migration image is always blurred and smoothed. In this situation, a more focused image with sharp boundaries of contrasting conductivities is often required. Portniaguine and Zhdanov [7] introduced focusing stabilizers that made it possible to recover models with sharp boundaries and contrasts. In this letter, we consider the minimum support (MS) and minimum vertical gradient support (MVGS) stabilizers [8]. The MS stabilizer promotes sharp boundaries in both vertical and horizontal directions, which is most appropriate for a blocky target. The MVGS stabilizer enforces the sharp boundaries in the vertical direction only, which is suitable for a layered target. In numerical studies presented below, the targets in Model 1 and in the case study have a thin-layered shape, which can be recovered by the MVGS stabilizer. The target in Model 2 has a blocky shape, which is suitable for the application of the MS stabilizer.

We solve the minimization problem (14) using the reweighted, regularized, conjugate gradient (RRCG) method, which is easier to implement numerically [6]. The problem can be solved quickly in a few iterations, thanks to the linearization of the Lippmann–Schwinger equation by introducing the modified conductivity.

After the modified conductivity, $m(\mathbf{r})$, is determined, we can find the conventional conductivity from (5) as follows:

$$\sigma_a(\mathbf{r}) = \frac{m(\mathbf{r})}{[1 + \lambda(\mathbf{r})]} \quad (15)$$

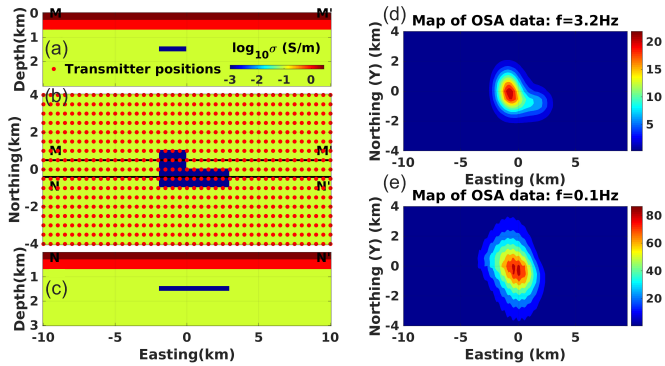


Fig. 1. Model 1 and maps of OSA data. (a) and (c) Cross sections of model 1 along profiles MM' and NN' , whose locations are indicated by black solid lines in (b). (b) Horizontal section of the model at a depth of 1.5 km. Red dots: transmitter positions for the synthetic survey. Note that (a)–(c) share the same abscissa. (d) and (e) Maps of amplitude of OSA data for the frequency components of 3.2 and 0.1 Hz.

where the reflectivity coefficient $\lambda(\mathbf{r}) = \mathbf{E}^a(\mathbf{r})/\mathbf{E}^b(\mathbf{r})$ and \mathbf{E}^a and \mathbf{E}^b are, respectively, anomalous and background fields in the anomalous domain, calculated based on (6).

In this letter, we apply the least squares migration to the OSA data, assuming that $\mathbf{d} = \mathbf{d}_R$ in (14). It is worth noting that one could apply migration directly to the observed inline E -field data. The advantage of applying migration to OSA data is threefold:

- 1) The data volume of OSA data is much smaller compared to the observed inline E -field data, which reduces the computation time significantly.
- 2) The OSA data can be computed using one SA source. The observed towed streamer data are generated by multiple positions of the moving transmitter, which makes the migration of the observed E -field data very computationally expensive.
- 3) The sensitivity of OSA data to the model parameters is focused within the area of target's location as a result of the optimal interference of the observed fields [as defined in (1)].

IV. SYNTHETIC MODEL STUDY

A. Model 1

The developed methods and computer code were tested using computer-generated data. Model 1 represents a three-layered geoelectrical model consisting of a 300 m sea-water layer with a conductivity of 3 S/m, the second 400-m layer of 1 S/m, and a 0.1 S/m half-space of the basement. An L-shaped hydrocarbon (HC) reservoir is embedded in the third layer with a depth of 1400 m to the top, as shown in Fig. 1. We set the conductivity of the reservoir to be 10^{-3} S/m, with a conductivity contrast ratio of 100 to the bedrocks. The towed streamer EM survey consists of 16 survey lines with 500-m line spacing running in the east direction. The horizontal electric dipole transmitter with a moment of 1000 Am is oriented in the east direction and is towed at a depth of 10 m from -10 to 10 km to the east. The shot interval is also of 500 m, with the locations of the transmitters denoted

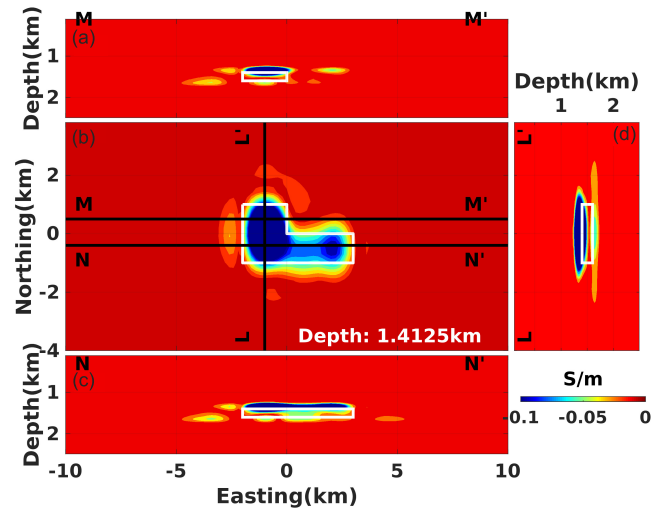


Fig. 2. Migration images of model 1. A horizontal section of the image at a depth of 1.41 km is shown in (b), with vertical profiles corresponding to MM' , NN' , and LL' (indicated by black solid lines) presented in (a), (c), and (d), respectively. The white solid lines outline the boundaries of the L-shaped reservoir. Note that (a)–(c) share the same abscissa, while (b) and (d) have the same ordinate.

TABLE I
RUN TIME FOR MODEL 1

Hardware	Run time
Intel Xeon Gold 6130	~ 500 s
Intel Xeon X5472	~1000 s

by red dots in Fig. 1. Twenty-five receivers with offsets from 1 to 7 km are towed at a depth of 100 m measuring the in line electric fields at eight frequencies between 0.1 and 3.1623 Hz. This frequency range corresponds to that typically used in the towed streamer surveys. The data were contaminated with 2% Gaussian noise.

We have applied the OSA method [4], [5] to the observed data. For every survey line, all the shots were combined to construct an OSA source for each virtual receiver location and frequency. Fig. 1(c) and (d) presents the maps of OSA data for all virtual receivers of two frequency components, respectively. The approximate horizontal location of the reservoir is recovered well.

We consider the OSA data as the observed data, $\mathbf{d} = \mathbf{d}_R$, and perform the least squares migration directly on them. To deal with the diffusive nature of the EM fields, the MVGS stabilizer was applied for the regularization. The migrated modified conductivity was then normalized to the conventional conductivity using (15). Fig. 2 presents the migration images. One can see that the location and shape of the reservoir are both well recovered horizontally and in the vertical direction. Note that, in this numerical experiment, we contaminated the data with some Gaussian noise. The minor conductivity fluctuations in the migration images in Fig. 2 are introduced by the noise in the data.

The run time of least squares migration for Model 1 is given in Table I.

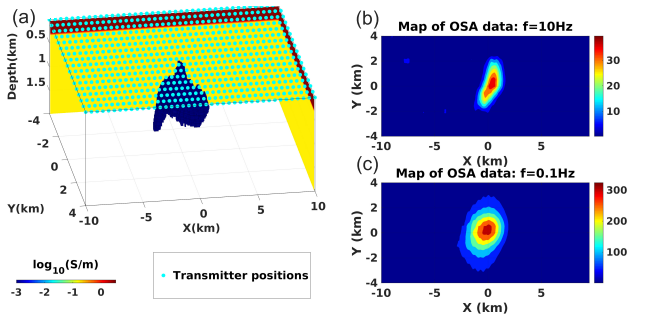


Fig. 3. (a) 3-D view of the salt dome model. The background is simplified into two-layered media, as shown in the vertical slices. We denote the transmitter positions for the synthetic survey with cyan dots. (b) and (c) Illustrate the maps of amplitude of OSA data for the frequency components of 10 and 0.1 Hz, respectively.

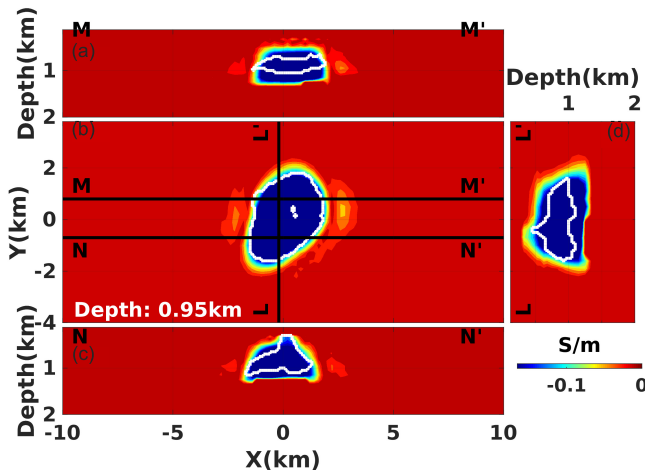


Fig. 4. Migration images of model 2. (b) A horizontal slice of the migration image at a depth of 0.95 km. (a), (c), and (d) Vertical profiles. Locations of the profiles in the map view are shown in (b). The boundaries of the salt dome are delineated by white solid lines.

B. Model 2

Model 2 is the SEG/EAGE Salt. For convenience, we simplified the model by considering a two-layered background: a 300-m, sea-water layer with a resistivity of $0.3 \Omega \cdot \text{m}$ and a $6\text{-}\Omega \cdot \text{m}$ half-space of sediments. The resistivity of the salt dome is set to $1000 \Omega \cdot \text{m}$, as shown in Fig. 3(a). The survey configuration is the same as in Model 1 except that the data are measured at eight frequencies between 0.1 and 10 Hz. The synthetic data were first contaminated with 1% Gaussian noise and imaged using the OSA method. As illustrated in Fig. 3(b) and (c), the OSA images are located at the salt dome horizontally well.

The produced OSA images were then migrated with the least squares migration with an MS stabilizer; the migrated modified conductivity was also normalized to conductivity as in a previous model study. One can see from Fig. 4 that the migration image recovers the location and shape of the salt body reasonably well. This result illustrates that the least squares migration can be used to image subsurface anomalies from the OSA data.

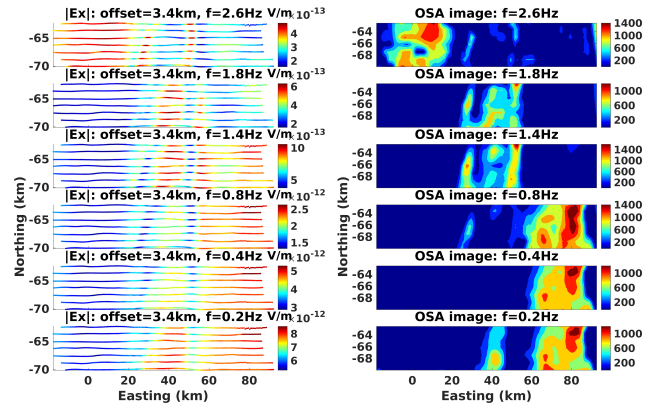


Fig. 5. (Left) Maps of amplitude of the observed inline electric field E_x at a common offset of 3.4 km for all six frequency components. (Right) Maps of amplitude of OSA data.

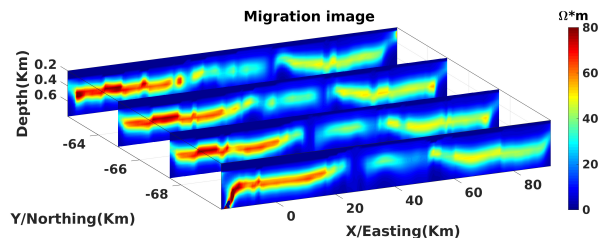


Fig. 6. 3-D view of migration image. A resistive layer with an anticline shape to the center of the survey area is recovered.

V. CASE STUDY

In this section, we present the results of application of the developed least squares migration method to the data collected by a TSEM survey conducted by Petroleum Geo-Services (PGS) in the Barents Sea. The TSEM data used in our numerical study were collected at seven survey lines at six frequencies of 0.2, 0.4, 0.8, 1.4, 1.8, and 2.6 Hz. The 8700-m-long EM streamer was towed at a depth of approximately 100 m below the sea surface. Twenty-three receivers with offsets between 2057 and 7752 m were selected. The electric current source was towed at a depth of approximately 10 m below the sea surface. Maps of observed inline electric field at a common offset of 3.4 km for all six frequency components are shown in Fig. 5.

We have applied the OSA method to the data for each frequency separately. The reference field was selected to be the set of the observed data generated by the remotely located transmitter for all frequencies, assuming that this field was least affected by the anomalous resistivity in the survey area. The OSA images are shown in Fig. 5.

We have migrated the OSA data using the developed least squares migration algorithm with the MVGS focusing and horizontal maximum smoothing stabilizers. The background model was chosen to be a two-layered model consisting of a 300 m sea-water layer with a resistivity of $0.33 \Omega \cdot \text{m}$ and of $5 \Omega \cdot \text{m}$ sea-bed half-space. The initial model was obtained by performing 1-D inversion of the data for the common transmitter–receiver middle point. As can be seen from the migration images (Fig. 6), there is a resistive layer at a depth of about 500 m. This layer bends up in the central part of the

survey area, forming an anticline structure, which coincides with that of the OSA image.

VI. CONCLUSION

We have developed a fast imaging method for interpretation of the TSEM data. The method consists of two steps. In the first step, we apply the OSA method to image the EM data observed at individual frequencies. In the second step, we use the migration transform of the OSA data jointly for all frequencies to generate the conductivity image of the seabottom formation. The migration is formulated as the inner product of the backward-propagated and forward-propagated EM fields generated by the OSA source. By linearizing the Lippmann–Schwinger integral equation, we were able to develop a rapid solver for both the backward-propagation and forward-modeling problems. We have also increased the sharpness of the inverse model by incorporating MS or MVGS regularization into the iterative migration. A synthetic test study demonstrated that the developed method could recover the horizontal location and the depth of the target reasonably well. The practical effectiveness of the method was also shown by imaging the TSEM data collected by PGS in the Barents Sea.

ACKNOWLEDGMENT

The authors acknowledge PGS for providing the field EM data. The authors also thank Dr. Zhenwei Guo and an anonymous reviewer for providing useful suggestions, which helped improving the manuscript.

REFERENCES

- [1] Y. Fan *et al.*, “Synthetic aperture controlled source electromagnetics,” *Geophys. Res. Lett.*, vol. 37, no. 13, Jul. 2010.
- [2] Y. Fan *et al.*, “Increasing the sensitivity of controlled-source electromagnetics with synthetic aperture,” *Geophysics*, vol. 77, no. 2, pp. E135–E145, Mar. 2012.
- [3] A. Knaak, R. Snieder, Y. Fan, and D. Ramirez-Mejia, “3D synthetic aperture and steering for controlled-source electromagnetics,” *Lead. Edge*, vol. 32, no. 8, pp. 972–978, Aug. 2013.
- [4] D. Yoon and M. S. Zhdanov, “Optimal synthetic aperture method for marine controlled-source EM surveys,” *IEEE Geosci. Remote Sens. Lett.*, vol. 12, no. 2, pp. 414–418, Feb. 2015.
- [5] M. S. Zhdanov, D. Yoon, and J. Mattsson, “Rapid imaging of towed streamer EM data using the optimal synthetic aperture method,” *IEEE Geosci. Remote Sens. Lett.*, vol. 14, no. 2, pp. 262–266, Feb. 2017.
- [6] M. S. Zhdanov, *Inverse Theory and Applications in Geophysics*, 2nd ed. Oxford, U.K.: Elsevier, 2015.
- [7] O. Portniaguine and M. S. Zhdanov, “Focusing geophysical inversion images,” *Geophysics*, vol. 64, no. 3, pp. 874–887, May 1999.
- [8] M. S. Zhdanov, *Foundations of Geophysical Electromagnetic Theory and Methods*, 2nd ed. Oxford, U.K.: Elsevier, 2018.